

Safety Diagnostic Tool for Non-Small Cell Lung Cancer (NSCLC) Lyophilized Serum

Abstract

The international protocol utilized in diagnosing non-small cell lung cancer (NSCLC) often yields inaccurate results due to limited diagnostic capability in the early stages. Carcinoembryonic Antigen (CEA), a well-known serum tumor marker used in NSCLC diagnosis, has restricted sensitivity and specificity. Despite this, it serves as a primary supplementary diagnostic tool that confirms findings from diagnostic radiology (PET-CT). Regrettably, its limited sensitivity fails to identify around one-third of NSCLC patients. With a growing number of patients being diagnosed with NSCLC, the effectiveness of the provided treatment is constrained. Therefore, there is an urgent need to discover, enhance, and establish a new technique that aids in the diagnosis of NSCLC. The low-angle x-ray scattering (LAXS) method was utilized to analyze the lyophilized serum of NSCLC patients, creating distinct patient profiles that identify molecular variances among NSCLC patients without subjecting them to harmful radiation exposure. The resulting LAXS profile exhibited two peaks, with the initial peak at 4.8° being particularly responsive to changes in protein structures, distinguishing them as the primary unique features compared to normal serum. By comparing LAXS profile measurements of NSCLC patients to those of individuals with normal serum, the specific 4.8° scattering peak emerged as a defining characteristic for distinguishing NSCLC patients from healthy individuals. Leveraging the LAXS technique provides comprehensive molecular insights, showing promise as a valuable tool for detecting NSCLC at an early stage.

Keywords: Low-angle X-ray scattering (LAXS) technique, Non-small cell lung cancer (NSCLC), Patient lyophilized serum, Diagnostic Tool

Introduction

In both industrialized and developing nations, cancer is ranked as the second disease after cardiovascular diseases in terms of mortality.^[1] Among cancer patients in the US,^[1, 2] China,^[3] and other countries, lung cancer is the most common cause of death, with the majority of patients diagnosed at an advanced age.^[4] Its histologic classification separates it into two primary subtypes: small cell lung cancer (SCLC) has a ratio of 15–20%,^[2, 5] whereas non-small cell lung cancer (NSCLC) is distributed among lung cancer patients by about 80–85% globally.^[1, 6] The 2017 clinical guidelines of the National Comprehensive Cancer Network (NCCN) state that less than one-fifth (17.7%) of patients with lung cancer are still alive five years following diagnosis.^[1] Patients with non-small cell lung cancer (NSCLC) typically experience late-stage symptoms before diagnosis; initial diagnoses are made based on clinical signs and bio-sample tests. Diagnoses are confirmed with

molecular diagnostic imaging (i.e., PET-CT, fMRI).^[2, 5-7] Several analytical platforms must be used in order to analyze diverse biological molecules for comprehensive NSCLC testing for several predictive indicators. The integration of several NSCLC molecular assays into a single diagnostic process is the subject of current studies.^[6] On the other hand, due to its suitable sensitivity to the treatment plan, histologic inspection and classification are important.^[2] Tumor markers, obtained either by histologic biopsy or serologic markers, are the primary means of diagnosing patients with this kind of cancer. These markers are then verified by radiological examinations (PET-CT).^[4, 5] Smokers are among the people with a higher chance of developing lung cancer. Twenty percent of the high-risk group has a higher surveillance rate due to undergoing the routine CT screening.^[7]

While the risk of unwanted radiation exposure is the primary barrier to CT screening for every patient, repeated

Mohammed Sayed Mohammed^{1*}, Asmaa Mohammed Sayed Mohammed^{2,3}

¹Department of Cancer Biology, National Cancer Institute, Cairo University, Cairo 11796, Egypt.

²Department of Biophysics, Faculty of Science, Cairo University, Giza 12613, Egypt. ³Unit of Medical Physics, Department of Radiotherapy, National Cancer Institute, Cairo University, Cairo 11796, Egypt.

Address for correspondence:

Mohammed Sayed Mohammed, Department of Cancer Biology, National Cancer Institute, Cairo University, Cairo 11796, Egypt. E-mail:

mohammed.sayed@nci.cu.edu.eg

Access this article online

Website: www.cci-j-online.org

DOI: [10.51847/qleIHBRpUP](https://doi.org/10.51847/qleIHBRpUP)

Quick Response Code:



How to cite this article: Sayed Mohammed M, Sayed Mohammed AM. Safety Diagnostic Tool for Non-Small Cell Lung Cancer (NSCLC) Lyophilized Serum. Clin Cancer Invest J. 2024;13(4):15-9. <https://doi.org/10.51847/qleIHBRpUP>

This is an open access journal, and articles are distributed under the terms of the Creative Commons Attribution-NonCommercial-ShareAlike 4.0 License, which allows others to remix, tweak, and build upon the work non-commercially, as long as appropriate credit is given and the new creations are licensed under the identical terms.

For reprints contact: Support_reprints@cci-j-online.org

© 2024 Clinical Cancer Investigation Journal

manipulation of the histologic biopsies is a challenge.^[8] Numerous biomarkers have surfaced as NSCLC predictive and prognostic markers.^[9-13] Early diagnosis of NSCLC clinical stage is critical for effective treatment, as late stages are associated with increased mortality and shorter survival.^[12-14] The fusion of ALK with oncogenes (e.g., echinoderm microtubule-associated protein-like 4) and rearrangements of the ROS1 gene, as well as inductive sensitization of EGFR mutations, are among the indicators involved in the prediction of NSCLC.^[9, 10] After EGFR TKI therapy for nine to thirteen months, patients with non-small cell lung cancer (NSCLC) and sensitizing EGFR mutations would likely become resistant to erlotinib, gefitinib, or afatinib as a form of chemotherapy.^[11, 14] The low-angle x-ray scattering (LAXS) approach was first demonstrated as a useful and promising biophysical tool with clinical sensitivity for identifying structural changes in lyophilized human serum two decades ago.^[15] Additionally, the production of a scattering peak using this method revealed more precise details about the induced molecular changes in the structural serum protein levels.^[15-17] Additionally, earlier research clarified the LAXS technique's sensitivity to track any changes in the molecular level structure in biological samples,^[15] distinguishing between characteristic profiles for normal and neoplastic breast tissues, and improving enhanced imaging methods.^[17] Additionally, it was applied to the tissues' discriminating criteria.^[18] Carcinoembryonic antigen (CEA), cytokeratin 19 fragments antigen (CYFRA21-1), and squamous cell carcinoma antigen (SCCAg) are the three tumor markers that are clinically approved for use in the diagnostic process of non-small cell lung cancer (NSCLC) when combined with histopathologic examinations, radiologic investigations, and PET-CT scanning.^[10] Even though histology is the most reliable indicator for diagnosing non-small cell lung cancer (NSCLC), the manipulation of surgical or biopsy specimens can compromise its accuracy.^[18] Molecular testing has become an essential part of NSCLC treatment. The detection of EGFR, BRAF, and MET mutations, as well as the analysis of ALK, ROS1, RET, and NTRK translocations, has already been incorporated into NSCLC diagnostic standards, and inhibitors of these kinases are now used routinely in clinical practice.^[16] For most of the previous two decades, therapeutic choices for individuals with stage III NSCLC remained largely unchanged. Over the last five years, ongoing advancements have coincided with advances in biomarker testing, innovative medicines, precision surgery, and radiotherapy, all of which are resulting in an increase in more individualized treatment options.^[19]

Scientists explore Circulating tumor cells (CTCs) which are a new but crucial indicator for cancer treatment. Because CTCs are rare, developing an effective mechanism for correctly quantifying them remains difficult.^[12, 13, 20]

Materials and Methods

Collection and preparation of patient's samples

The regulations and rules of the Egyptian National Cancer Institute (NCI) Cairo University governed this study for one

year. Ethical approval—including patient consent—for this study was not necessary, due to the patient samples and their data being taken from the routine clinical investigations from the departments of clinical pathology and diagnostic radiology as anonymous samples. After that, their clinical data results and residual samples were collected anonymously to protect the patients' rights. Blood samples were collected from 50 samples; 10 samples were healthy individuals (5 males and 5 females), 10 samples were diagnosed as high-risk group patients (seven males and three females), and 30 were diagnosed as NSCLC patients (25 males and five females). The NCI clinicians diagnosed NSCLC patients according to the National Comprehensive Cancer Network (NCCN) version 5, 2017,^[1] routine clinical investigations, tumor markers, and diagnostic radiology were performed, and the results were collected to compare with the LAXS technique. Internationally, the NSCLC distribution according to sex is different from Egypt, where females are not predominant, which is due to the high-risk group mainly men (smokers). The distribution of the age of the collected samples for the three groups was lightly matched. There were no patients suffering from NSCLC below 40 years of age, and it started to increase for samples of patients above 40 years up to 69 years of age. The whole clinical data for each group is illustrated in **Table 1**. The thirty NSCLC patients were classified according to their tumor grading; 8 patients (grade I), 17 patients (grade II), and 5 patients (grade III), whereas no grade IV NSCLC patients were included in this study. The patient samples in this study were collected via venipuncture process and were clotted at 37 °C temperature for half an hour. Following this, the blood samples were centrifuged for ten minutes at 5040× g (3000 rpm). Then, the supernatant patients' sera were separately collected and kept at -80 °C. According to previous research, which was elucidated, the suitable temperature for storing biological samples for long periods was -80 °C, and this condition did not affect the characteristic scattering behavior.^[15] The collected samples were lyophilized by using a freeze dryer (Edwards, UK) at minus fifty Celsius and negative vacuum pressure of 6.4 mbar in magnitude for six hours to complete water removal from the samples and then were kept in dry sealed plastic tubes at minus eighty Celsius. For LAXS measurements, the samples had to warm up at room temperature.

Table 1. Clinical data of investigated groups.

	Control	High Risk Group (Smokers)	NSCLC Group
	(n = 10)	(n = 10)	(n = 30)
Mean age (years)	42 ± 3.5	48 ± 3.1	50 ± 9
Sex:			
M	5	7	25
F	5	3	5
UICC stage:			
I	-----	-----	8
II	-----	-----	17
III	-----	-----	5

Measurements of X-ray scattering

The lyophilized powdered serum was smeared on glass mounted vertically in the rotating holder of the Shimadzu X-ray diffractometer to investigate the scattering profile of each individual. The operating condition of this instrument was working in reflection geometry at 40 kV and 30 mA, using a copper target to produce the mainly high collimated 8.047 keV X-ray beam. The scattering angles were investigated in this study from 2° up to 30°, with steps of 0.25°. The rotation was in (θ–2θ) mode. Sodium iodide crystal with a graphite monochromator in a scintillation detector collected the scattering data and interfaced to the computer.

Calculation and analysis of the parameters from the LAXS data profile

Table 2 presents the characterized parameters that were calculated from the LAXS profiles of the patient’s sera. **Figure 1** elucidated the calculation processes of these parameters. The first parameter was the full width at half maximum for the first and second peaks, which were acronymically known as FWHM1 and FWHM2, which had the scattering degrees 4.8° and 10.5°, respectively.

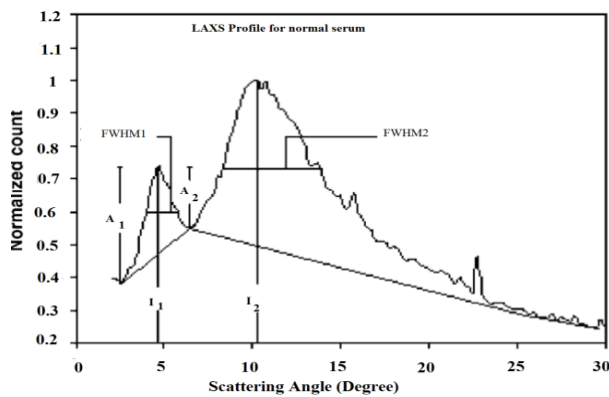


Figure 1. The calculation of the characterized parameters measured from the scattering profile of normal serum.

To estimate FWHM, the baseline for each peak was plotted, which made references to calculate their values, as illustrated in **Figure 1**. The percentage ratio of the first and second scattering peak values ($I_1/I_2\%$) was inserted in **Table 2**. Moreover, the amplitudes of the rising and falling edges of peaks 1 and 2 were tabulated to represent their values as A_1 and A_2 , respectively.

The final manipulated procedure for the characterized measured parameters was statistically analyzed by using the Statistical Package for the Social Sciences (SPSS) version 24. The representing forms of our data were tabulated as mean \pm standard error of the different parameters (**Table 2**). The analysis of variance (ANOVA) test was used to compare the mean values of each characterized parameter. Individual values for each parameter were used to calculate means. When the compared groups were statistically significant, an additional test was followed by Duncan’s multiple range test to test the discrimination of the investigated groups.

According to the World Health Organization (WHO) classification, NSCLC is distributed by more than 80% of lung cancer patients;^[1, 6] moreover, the latent diagnosis of NSCLC is mainly a medical problem due to the advanced cancer stage. While the routine medical investigation is dependent on general signs and symptoms in addition to laboratory markers, the results from these findings are diagnostically supported by radiologic imaging (PET/CT scan, brain MRI).

Results and Discussion

The LAXS-characterized parameters are shown in **Figure 1** for the normal sample. The high-risk group and NSCLC samples are presented in **Table 2**.

Table 2. The average values of the measured parameters for normal, high-risk group, and NSCLC serum sample low-angle X-ray scattering scanning data.

	Normal Serum (n = 10)	High Risk Group (n = 10)	NSCLC (n = 30)	F-Ratio	p-Value
FWHM ₁ (deg)	1.96 ± 0.12 ^a	1.95 ± 0.2 ^a	2.19 ± 0.20 ^b	4.906	0.0120
FWHM ₂ (deg)	5.23 ± 0.14	5.24 ± 0.22	5.39 ± 0.26	1.898	0.1600 ^c
Peak position ₁ (deg)	4.78 ± 0.15 ^a	4.93 ± 0.22 ^b	5.08 ± 0.16 ^b	8.515	0.0005
Peak position ₂ (deg)	10.52 ± 0.16 ^{a,b}	10.45 ± 0.22 ^a	10.62 ± 0.13 ^b	3.878	0.0270
$I_1/I_2\%$	55.14 ± 2.32 ^a	54.20 ± 1.42 ^{a,b}	53.10 ± 1.74 ^b	3.324	0.0440
$A_2/A_1\%$	45.64 ± 5.80 ^a	38.20 ± 3.82 ^b	33.80 ± 3.81 ^b	11.411	0.0001
Counts under peak ₁	7.12 ± 0.22 ^a	6.99 ± 0.16 ^a	6.62 ± 0.19 ^b	20.112	0.0001

^a Statistically classified group a.

^b Statistically classified group b which is significantly different to group a.

^c NS: non-significant.

All graphs were normalized to unify at the second peak of scattering at 10.5° to make them easily comparative and applicable. A maximum three-point average was then plotted

for each graph. The analysis of this investigation revealed two quite broad scattering peaks, as shown in **Figure 2**, while the presence of NaCl crystals in the serum sample resulted in

the presentation of several acute diffraction peaks.^[16] The distinct peak amplitudes varied based on the NaCl contents of the separate samples. A summary of **Figure 2** indicates distinct variations between the NSCLC and normal people in the first peak at 4.8° .

The full width at the half maximum of peak one ($FWHM_1$) for the NSCLC group is tabulated in **Table 2**, which also includes the estimated parameters. Notably, this value was higher than that of the normal and high-risk groups. There was no discernible difference between the high-risk and normal groups. Additionally, the initial scattering peak position showed a considerable shift, going from 4.8° for healthy individuals to 4.9° for the high-risk group and up to 5.1° for the NSCLC samples. In both the high-risk and NSCLC groups, the shift difference was not statistically significant (**Table 2**).

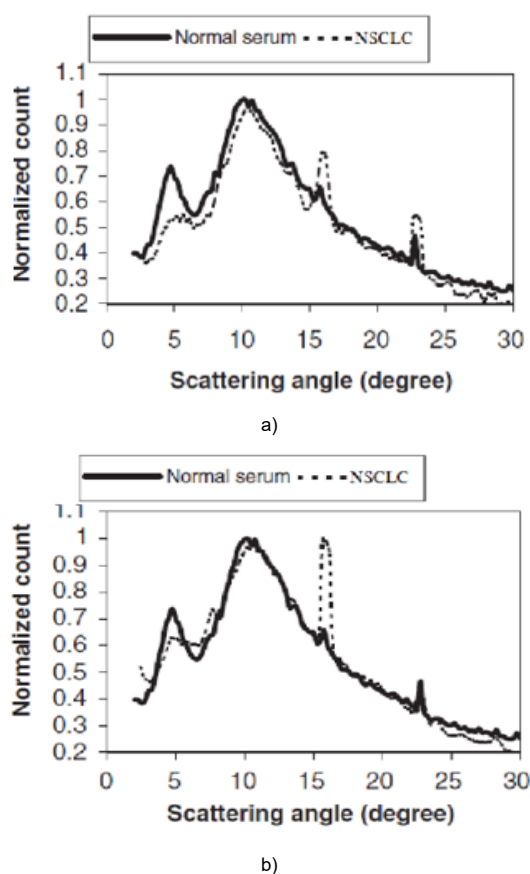


Figure 2. Comparison of NSCLC LAXS profiles to those of normal individuals.

In comparison to the healthy group, the NSCLC and high-risk groups showed a few declines in the percentage of the amplitude ratio of the first to second peaks ($I_1/I_2\%$). There was only one notable difference found between the high-risk and healthy groups. Peak 1 was made up of two edges: A_1 (rising) and A_2 (falling). The dividing ratio (A_2/A_1) that resulted was given in percentage form in **Table 2**. Because it combined the first peak's dropping edge with the second scattering peak, which caused the height A_2 to be lower than A_1 , this peak exhibited a unique its behavior. A substantial

difference between the normal and NSCLC groups with a large standard error is represented by the percentage ratio of (A_2/A_1). **Table 2** shows that the high-risk group's percentage ratio of (A_2/A_1) was significantly different from the healthy group and fell between the normal and NSCLC categories. **Figure 2** depicts the form of the initial sampling peak, which revealed that all NSCLC samples had a distinct shape from the normal samples.

The initial scattering peak was distorted in all NSCLC profiles, despite variations in peak form in each sample. NSCLC profiles typically showed a decrease in the area under the first peak compared to the health group profile. The NSCLC group had significantly lower numbers under peak one compared to the healthy group. **Table 2** provides a tabulated representation of this parameter.

This study found that six characterization factors were significantly different in two out of three groups. **Table 2** shows that $FWHM_2$ diversity was non-significant across all groups. The normal and NSCLC groups showed substantial variations in metrics such as $FWHM_1$, peak position 1, ($I_1/I_2\%$), ($A_1/A_2\%$), and counts beneath peak 1.

Two parameters, peak position one and ($A_2/A_1\%$), were used to differentiate between healthy and high-risk groups. Three parameters, $FWHM_1$, peak position two, and counts under peak one, revealed significant differences between NSCLC and high-risk groups. Previous investigations have verified the susceptibility of the first peak of scattering to protein structural changes,^[18, 19] which may explain the observed changes in the described parameters across all groups. Previous research found that irradiated serum's first scattering peak was distorted. The observed disparities in described parameters did not show a significant link with age in the investigated groups.

The LAXS technique addresses the issue of erroneous data in diagnosing and treating NSCLC, which is caused by lung tissue motions during breathes, particularly in early stages (tumor location and size).^[16] To address this clinical issue, the four-dimensional computed tomography (4DCT) technology captures respiratory motion and generates unique dynamic data for each patient. The analysis of 4DCT images in NSCLC patients shows a substantial association with tumor size, location, and clinical stage.^[19, 20] The LAXS approach is simpler than the 4DCT and does not expose patients to radiation. Furthermore, it is highly accurate regardless of tumor location or size.

Conclusion

Under the National Institutes of Health (NIH) rules; LAXS is a reliable biomarker due to its objective characterization, evaluation, unique indication of normal biologic processes, and ability to identify pathogenic processes. Additionally, clinical decision-making can be enhanced. The LAXS approach is a cost-effective, specific, and durable option for

NSCLC patients. It also minimizes the radiation risk associated with traditional radiologic studies.

Acknowledgments

None.

Conflict of interest

None.

Financial support

None.

Ethics statement

None.

References

1. Ettinger DS, Wood DE, Aisner DL, Akerley W, Bauman J, Chirieac LR, et al. Non-small cell lung cancer, version 5.2017, NCCN clinical practice guidelines in oncology. *J Natl Compr Canc Netw*. 2017;15(4):504-35.
2. Duma N, Santana-Davila R, Molina JR. Non-small cell lung cancer: Epidemiology, screening, diagnosis, and treatment. *Mayo Clin Proc*. 2019;94(8):1623-40.
3. Zhan S, Wang L, Wang W, Li R. Insulin resistance in NSCLC: Unraveling the link between development, diagnosis, and treatment. *Front Endocrinol (Lausanne)*. 2024;15:1328960.
4. Silvestri GA, Gould MK, Margolis ML, Tanoue LT, McCrory D, Toloza E, et al. Noninvasive staging of non-small cell lung cancer: ACCP evidenced-based clinical practice guidelines (2nd edition). *Chest*. 2007;132(3 Suppl):178S-201S.
5. Christofyllakis K, Monteiro AR, Cetin O, Kos IA, Greystoke A, Luciani A. Biomarker guided treatment in oncogene-driven advanced non-small cell lung cancer in older adults: A young international society of geriatric oncology report. *J Geriatr Oncol*. 2022;13(8):1071-83. doi:10.1016/j.jgo.2022.04.013
6. World Health Organization. Cancer. Available from: <https://www.who.int/news-room/fact-sheets/detail/cancer> (accessed on 19 January 2023).
7. De Wever W, Vankan Y, Stroobants S, Verschakelen J. Detection of extrapulmonary lesions with integrated PET/CT in the staging of lung cancer. *Eur Respir J*. 2007;29(5):995-1002.
8. Imyanitov EN, Iyevleva AG, Levchenko EV. Molecular testing and targeted therapy for non-small cell lung cancer: Current status and perspectives. *Crit Rev Oncol Hematol*. 2021;157:103194. doi:10.1016/j.critrevonc.2020.103194
9. Zamay TN, Zamay GS, Kolovskaya OS, Zukov RA, Petrova MM, Gargaun A, et al. Current and prospective protein biomarkers of lung cancer. *Cancers (Basel)*. 2017;9(11):155. doi:10.3390/cancers9110155
10. Liu L, Teng J, Zhang L, Cong P, Yao Y, Sun G, et al. The combination of the tumor markers suggests the histological diagnosis of lung cancer. *Biomed Res Int*. 2017;2017:2013989.
11. Li Y, Juergens RA, Finley C, Swaminath A. Current and future treatment options in the management of stage III NSCLC. *J Thorac Oncol*. 2023;18(11):1478-91.
12. Wang J, Liu X, Li J, Chen W. Digital circulating tumor cells quantification. *Anal Chem*. 2024;96(18):6881-8.
13. Cao R, Zhang M, Yu H, Qin J. Recent advances in isolation and detection of circulating tumor cells with a microfluidic system. *Se Pu*. 2022;40(3):213-23 [In Chinese].
14. Seijo LM, Peled N, Ajona D, Boeri M, Field JK, Sozzi G, et al. Biomarkers in lung cancer screening: Achievements, promises, and challenges. *J Thorac Oncol*. 2019;14(3):343-57. doi:10.1016/j.jtho.2018.11.023
15. Elshemey WM, Desouky OS, Mohammed MS, Elsayed AA, el-Houseini ME. Characterization of cirrhosis and hepatocellular carcinoma using low-angle x-ray scattering signatures of serum. *Phys Med Biol*. 2003;48(17):N239-46. doi:10.1088/0031-9155/48/17/401
16. Desouky OS, Elshemey WM, Selim NS, Ashour AH. Analysis of low-angle x-ray scattering peaks from lyophilized biological samples. *Phys Med Biol*. 2001;46(8):2099-106.
17. Elshemey WM, Desouky OS, Ashour AH. Low-angle X-ray scattering from lyophilized blood constituents. *Phys Med Biol*. 2001;46(2):531-9.
18. Howlader NN, Noone AM, Krapcho M, Garshell J, Miller D, Altekruse SF, et al. SEER Cancer Statistics Review, 1975–2013, Based on November 2015 SEER Data Submission, Posted to the SEER Web Site, April 2016; National Cancer Institute: Bethesda, MD, USA, 2016.
19. Li H, Dong L, Bert C, Chang J, Flampouri S, Jee KW, et al. AAPM task group report 290: Respiratory motion management for particle therapy. *Med Phys*. 2022;49(4):e50-81. doi:10.1002/mp.15470
20. Chen ZQ, Huang LS, Zhu B. Assessment of seven clinical tumor markers in diagnosis of non-small-cell lung cancer. *Dis Markers*. 2018;2018:9845123. doi:10.1155/2018/9845123